Dead-time Compensation Based on Pole Voltage Measurement

Seung-Jun Chee, Jaesuk Kim and Seung-Ki Sul
Department of Electrical and Computer Engineering
Seoul National University
Seoul, Korea
cheesj80@eepel.snu.ac.kr, kimjs@eepel.snu.ac.kr and sulsk@plaza.snu.ac.kr

Abstract*— This paper presents a simple dead-time compensation method for a three phase PWM inverter based on the measured pole voltage using enhanced capture (eCAP) module usually embedded in a digital signal processor (DSP). The information of the inverter pole voltages can be employed to compensate the voltage difference between commanded voltage and actual output voltage of the PWM inverter. Because the method does not rely on any other information except for the measured switching instants of each phase of the inverter, it can be easily accommodated into the low cost drive system where accurate and instantaneous measurement of the phase current is not available. The difference can be added at the next sampling time of the switching period of the PWM and could be updated after one sampling period due to the digital sampling delay. These total two sampling periods delay would degrade the performance of the dead-time compensation. To enhance the performance, a PI regulator is employed to nullify the difference in controlled manner. The effectiveness of the proposed compensation methods has been verified through the experimental results. Through the proposed compensation method, the 5th and 7th harmonic currents are reduced by 85% and 70%, respectively.

I. INTRODUCTION

The three phase PWM voltage source inverter topology using 6 active switches, shown in Fig. 1, is widely used in DC to AC power conversion such as the adjustable speed drive and the grid-tied power conversion, owing to the simple structure and easiness in the control.

To avoid the shoot-through phenomenon during commutation of switches of each phase of the inverter, both active switches are turned off for a while. This turn-off time period is so called dead-time or blanking time. During the dead-time, the output pole voltage is determined by the polarity of the corresponding current which is flowing through the anti-parallel diode of each switch.

The dead-time and its effect on the pole voltage are conceptually shown in Fig. 2. In a case of the positive phase current as shown in Fig. 2. (a), there exist two dead-time ranges during the switching period (T_{sw}). When a carrier wave is decreasing, the pole voltage is $-V_{dc}/2$ during the dead-time because the current is flowing thorough the bottom anti-

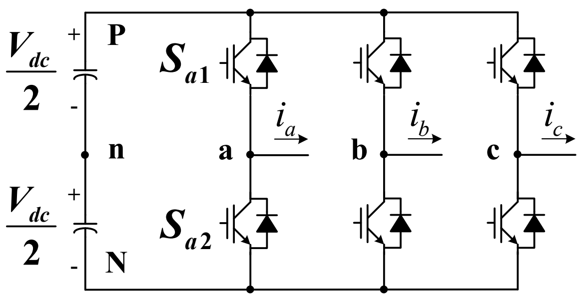

Fig. 1. 3 phase PWM inverter

parallel diode. So there is no distortion in the pole voltage. However, when a carrier wave is increasing, the pole voltage is still $-V_{dc}/2$ during the dead-time. Then, the pole voltage distortion occurs because the pole voltage is still $-V_{dc}/2$ during dead-time when desirable value is $V_{dc}/2$. If the phase current is positive, the average value of the real pole voltage during T_{sw} would be smaller than the desired reference pole

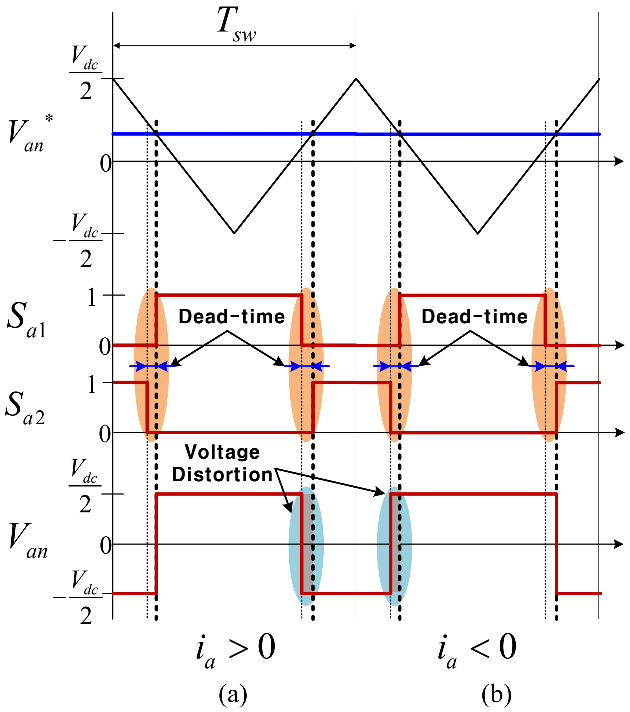

Fig. 2. Dead-time (T_{dead}) and its effect on pole voltage (a) $i_a > 0$, and (b) $i_a < 0$

978-1-4673-7151-3/15/$31.00 ©2015 IEEE

voltage. Otherwise, the average value would be larger than the reference pole voltage. Thus the dead-time results in the voltage distortion of the pole voltages which causes low order harmonic components in the output current of the inverter [1]. To avoid the problems mentioned above, there were many efforts for the dead-time compensation [1-12]. Most of them exploit the phase current information under the assumption of accurate and instantaneous measurement of the current.

In most of low cost drive intended for pump and fan drive, the instantaneous and accurate measurement of the current is not available. Also, even in the case of some drives with phase current measurement, the information would not be accurate enough to compensate the dead-time effect because of the offset and the delay in the measured phase current.

In this paper, by using a simple time measurement function so called an eCAP module embedded in most of conventional digital signal processor (DSP), the switching instants of each pole of the inverter can be measured accurately and instantaneously. Based on the measured switching instants, the actual pole voltage can be calculated and compared to the desired reference pole voltage. The differences between two voltages are used to compensate the dead-time effect of the inverter.

II. Proposed Voltage Measurement Method

If the actual pole voltage information can be acquired, it could be used for the compensation of the dead-time effect. The voltage can be obtained by measuring the PWM inverter output voltage directly [13-16]. By simply integrating each pole voltage of the inverter during a sampling period, the average output voltage for a sampling period can be measured at the end of each sampling period of the PWM. It would be the most accurate method in principle, but it needs an additional circuitry and control logic [14].

In this paper, a simple voltage-sensing circuit is devised based on time measurement module embedded in most of DSPs. The conceptual circuit for the proposed voltage measurement method is shown in Fig. 3 (a), where a voltage divider and comparator are connected to the each phase of the inverter and the output of the comparator is connected to eCAP pin of a DSP, which is a time measurement module of a DSP used in this paper. In this circuit, the threshold voltage (V_{th}) of the comparator is assumed as a half of the dc-link voltage. The actual pole voltage of each phase can be calculated by the switching instants (T_{on} in Fig. 3 (b)) of the pole voltage of the inverter, stored in eCAP module. Most of the DSP chips used in motor drive system contain such capture modules in them. The proposed circuit is implemented on control board as shown in Fig. 3 (c). From (1) and (2), the actual average pole voltage during a switching period can be calculated. Through this calculation, the average pole voltage can be obtained at the end of the sampling period under the assumption that dc-link voltage is constant for the sampling period and that there is no voltage drop on the switching devices. The assumption would be valid in most of the

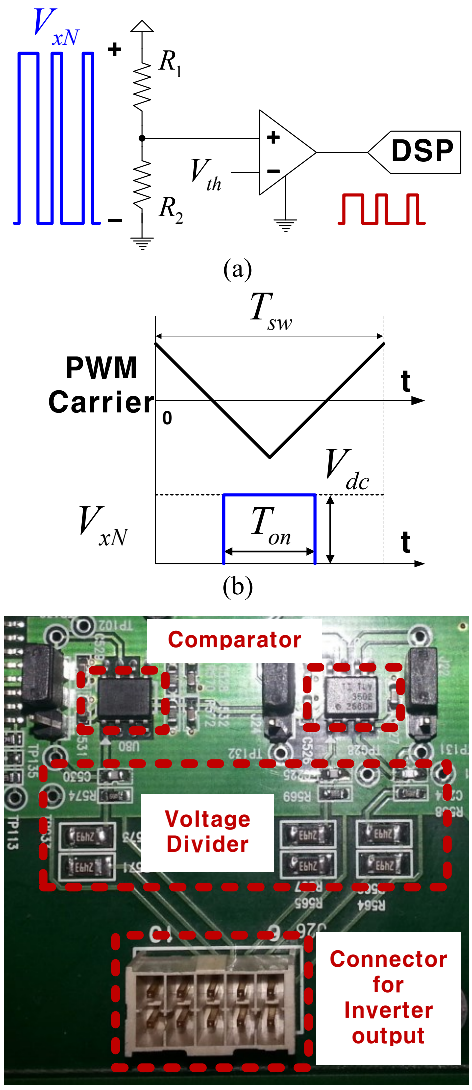

(a) (b) (c)

Fig. 3. The voltage measurement (a) conceptual circuit, (b) waveforms of $\boldsymbol{V_{xN}}$ with a PWM carrier, and (c) voltage sensing circuit on PCB

operating condition of the inverter except for the operation with very small dc-link capacitance and low modulation index.

$$\overline{V_{xN}} = \frac{1}{T_{sw}} \int_{kT_{sw}}^{(k+1)T_{sw}} V_{xN} dt = \frac{1}{T_{sw}} \int_{T_{on}} V_{xN} dt$$

$$= V_{dc} \frac{T_{on}}{T_{sw}} \ (where\ x = a, b, c) \quad (1)$$

$$V_{xn}{}^{cap} = \overline{V_{xN}} - \frac{V_{dc}}{2} \quad (2)$$

III. Proposed Dead-Time Compensation Method (DTCM)

The basic principle of the dead-time compensation is calculating the difference ($V_{xn}{}^{**diff}$) between the reference pole voltage ($V_{xn}{}^{**}$) and the actual pole voltage ($V_{xn}{}^{cap}$) at the end of each sampling period, and adding the difference value to the next pole voltage ($V_{xn}{}^{*}$) in the starting point of the next

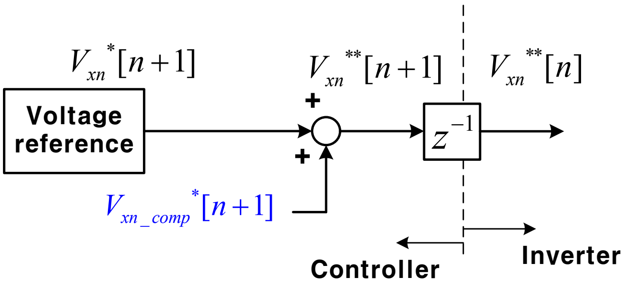

Fig. 4. Block diagram of general DTCM

sampling period. However, the compensation cannot be done instantaneously because of the digital delay of the PWM logic. It can be implemented as the block diagram shown in Fig. 4.

The difference is calculated by (3). The compensation voltage value can be represented as (4) in Fig. 4.

$$V_{xn}{}^{**diff}[n] = V_{xn}{}^{**}[n] - V_{xn}{}^{cap}[n] \quad (3)$$

$$V_{xn\_comp}{}^{*}[n+1] = V_{xn}{}^{**diff}[n-1] \quad (4)$$

This direct compensation method is called as "DTCM1" in this paper. From (4), the compensation would be done after two sampling periods because of one digital sampling delay and additional one sampling period delay due to the PWM update.

The simulation of the proposed DTCM1 is implemented based on an induction motor drive system with parameters in Table I. The motor is controlled by constant V/F operation (154V/50Hz). The dc-link voltage, switching frequency and dead-time are set as 320 V, 20 kHz, and 3 μs, respectively. The sampling frequency is 20 kHz, which is the same as the switching frequency. The load torque, which is proportional to the square of the rotational speed, is applied to the target induction motor by a load machine.

In Fig. 5 (a), the phase current is highly distorted without dead-time compensation method. However, when the DTCM1 is applied, the distortion of the phase current is conspicuously reduced as shown in Fig. 5 (b). Additionally, the fundamental component of the current is also reduced, thanks to the increased fundamental component of the pole voltage through the compensation.

But from the FFT results of the phase current in Fig. 6, 5th,

TABLE I. PARAMETERS OF INDUCTION MOTOR

Item	Value	Unit
P_{rated}	3.7	kW
Pole number	4	
R_s	0.22	Ω
R_r	0.3	Ω
L_m	63.62	mH
L_{ls}	2.4	mH
L_{lr}	2.4	mH

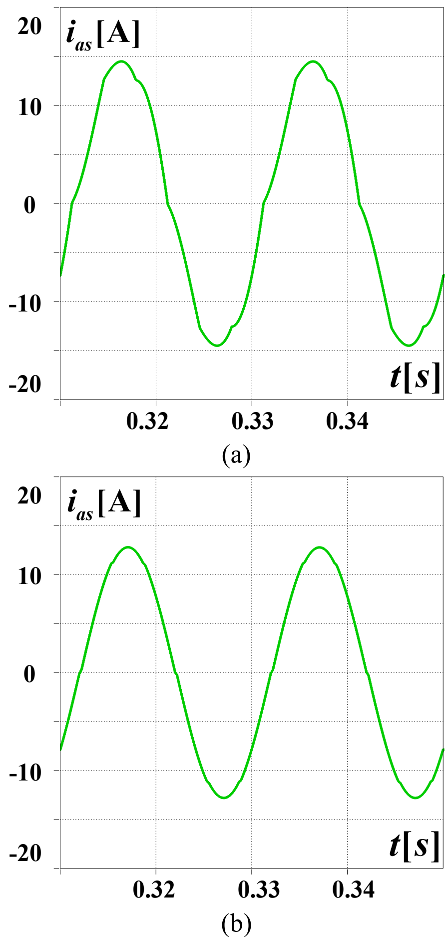

Fig. 5. Simulation results – Phase current (a) without dead-time compensation method, and (b) with DTCM1

7th harmonic components of the current still exist even though the DTCM1 has been used. It is because the compensation voltage is based on the voltage which has 2 sampling time delay as (4). So $V_{xn}{}^{*diff}$ defined as (5) is inevitably not zero near zero crossing point of each phase current as shown in Fig. 7.

$$V_{xn}{}^{*diff}[n] = V_{xn}{}^{*}[n] - V_{xn}{}^{cap}[n] \quad (5)$$

If the dead-time compensation is done instantaneously without any delay, $V_{xn}{}^{*diff}[n]$ should be zero all the time.

In this paper, another DTCM employing a Proportional and Integral (PI) regulator is proposed as shown in Fig. 8, and is called "DTCM2". If $V_{xn}{}^{*diff}$ is not zero, in addition to the direct compensation of the voltage difference the PI regulator tries to nullify the difference. The final output of the regulator is $V_{xn\_comp}{}^{*}$. And $V_{xn}{}^{**diff}$ which is used for direct compensation voltage for the DTCM1 is utilized as a feed-forwarding term. And, the DTCM2 is exactly the same as the DTCM1 when the PI gains are set as zero.

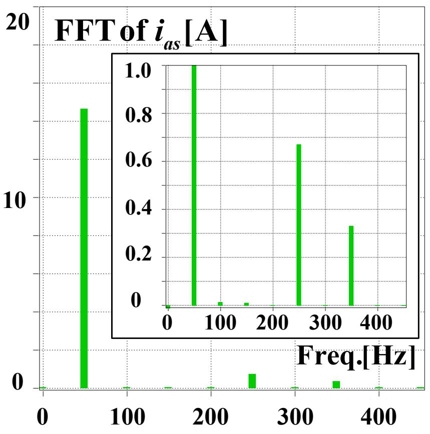

(a)

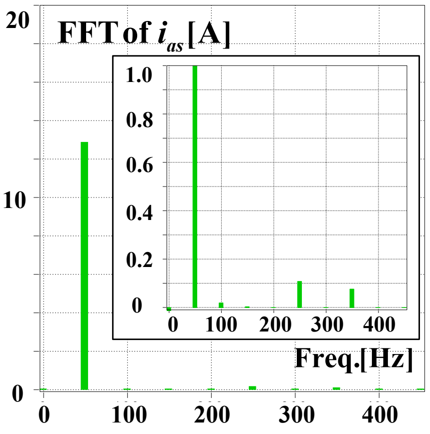

(b)

Fig. 6. Simulation results – FFT of phase current in Fig. 5 (a) without dead-time compensation method, and (b) with DTCM1

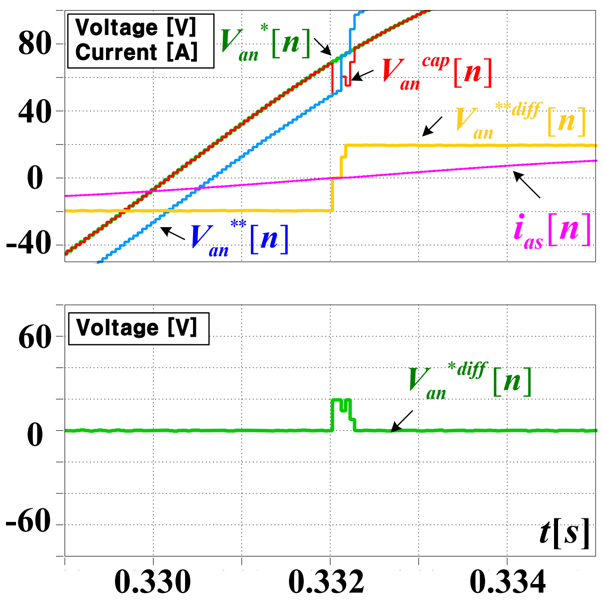

Fig. 7. Simulation result of DTCM1 – initial commanded voltage (V_{an}^{*}), final commanded voltage (V_{an}^{**}), measured voltage by eCAP (V_{an}^{cap}), initial voltage difference (V_{an}^{*diff}) and final voltage difference (V_{an}^{**diff}) near the phase current's zero-crossing

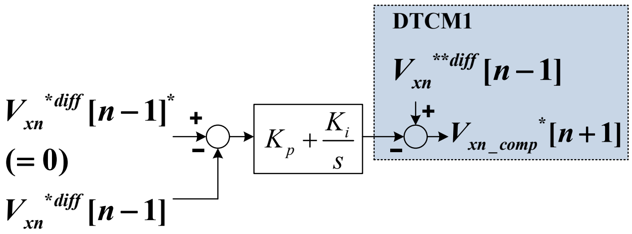

Fig. 8. Block diagram of DTCM2

The z-domain transfer function ($G[z]$) between V_{xn}^{*diff} and V_{xn_dead} can be derived as (6), where V_{xn_dead} is the distortion voltage caused by the dead-time. It is desirable for $G[z]$ to be as small as possible. If the dead-time compensation method is not applied, $G[z]$ would be unity and is defined as G_{wo_DTCM}.

$$G[z] = \frac{V_{xn}^{*diff}[n]}{V_{xn\_dead}[n]} \quad (6)$$

If the DTCM1 is applied, $G[z]$ is represented as (7) and is defined as G_{DTCM1}.

$$G[z] = \frac{z^2-1}{z^2} \quad (7)$$

If the DTCM2 is applied, $G[z]$ is represented as (8) and is defined as G_{DTCM2}.

$$G[z] = \frac{z^3-z^2-z+1}{z^3-z^2+(K_p+T_{sw}K_i)z+(-K_p)} \quad (8)$$

The Bode plots of G_{WO_DTCM}, G_{DTCM1} and G_{DTCM2}, whose Proportional and Integral gains are 0.4 and 400 respectively, are shown in Fig. 9. When the DTCM2 is applied with these gains, it can be seen that the harmonic components over 2 kHz would be slightly amplified but that the harmonic components below 2 kHz would be conspicuously reduced with DTCM2.

In Fig. 10, the simulation results of the DTCM2 with the

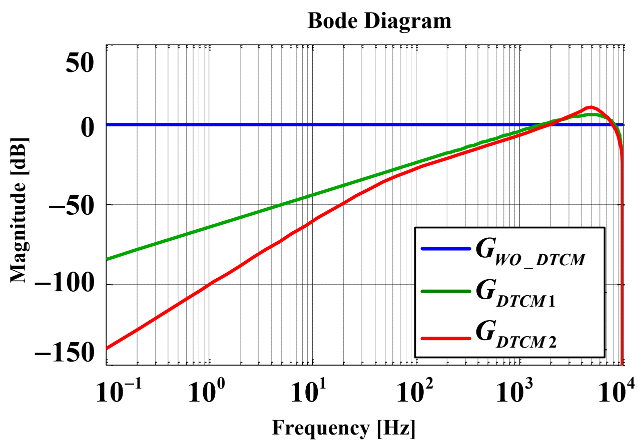

Fig. 9. Bode plot of $G[z]$

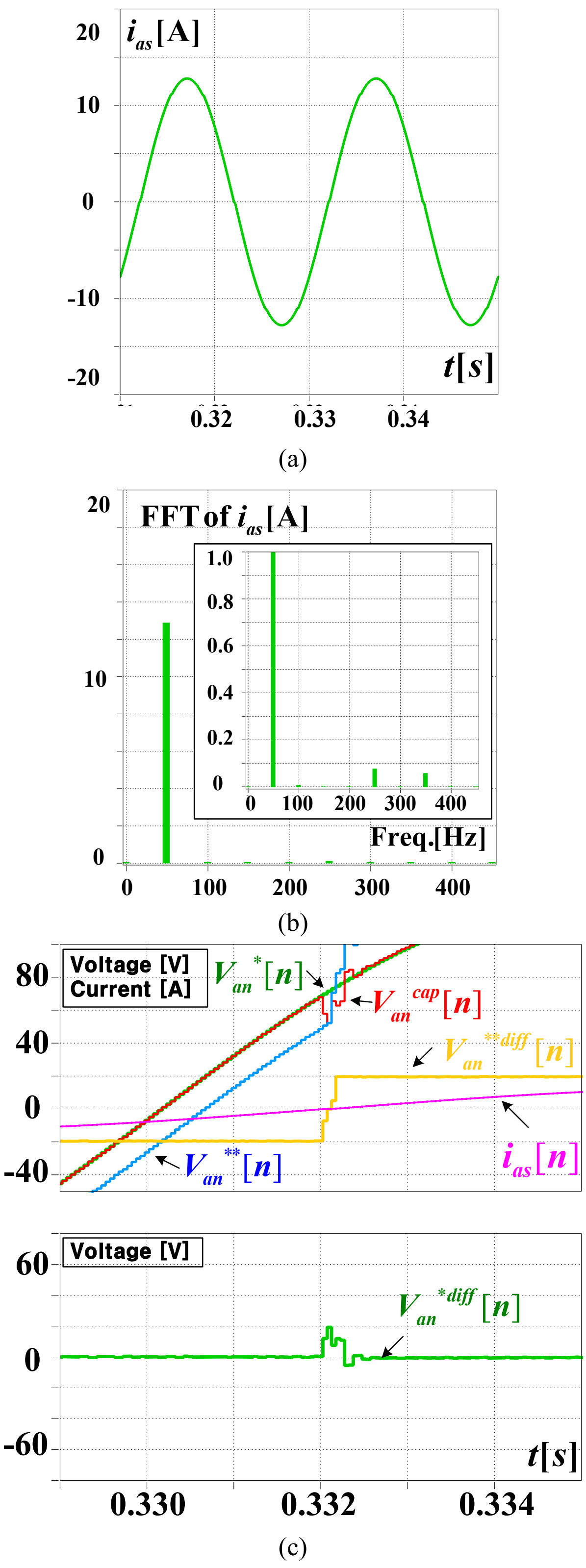

(c)

Fig. 10. Simulation results of DTCM2 (a) phase current, (b) FFT of phase current, and (c) various voltages and current near zero current

same operating condition in Fig. 5 are shown when the PI gains are 0.4 and 400, respectively. Compared to the results

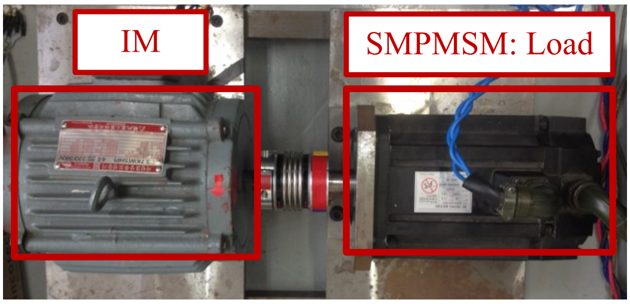

Fig. 11. Experimental setup

with DTCM1 in Fig. 6 (b), the 5[th], 7[th] harmonic components of the phase current in Fig. 10 (b) are diminished as expected in Bode plot.

IV. Experimental Results

The experimental set-up for the verification of the proposed

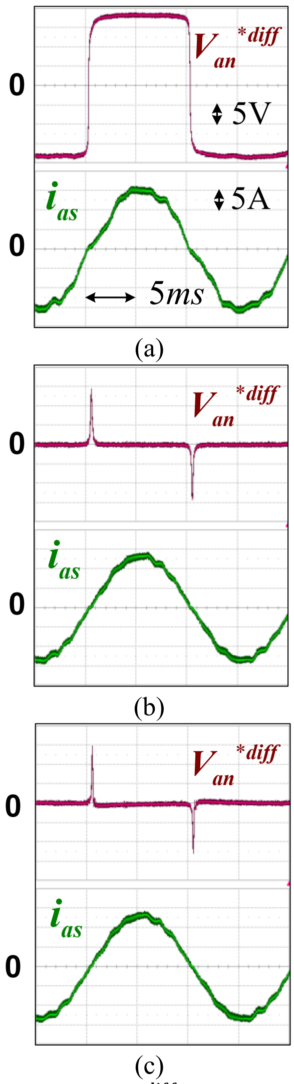

Fig. 12. Experimental result - V_{an}^{*diff}, i_{as} (a) without DTCM, (b) with DTCM1, (c) with DTCM2

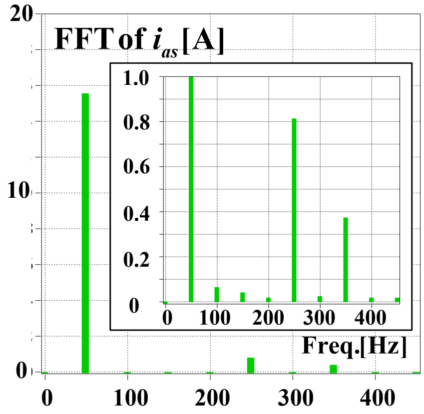

(a)

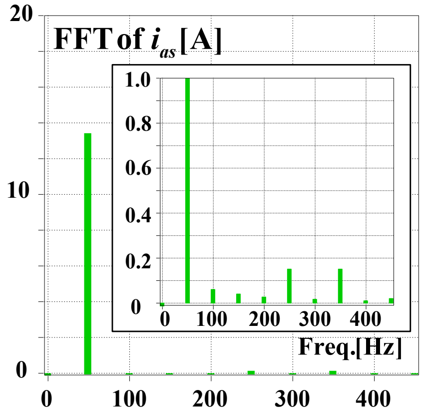

(b)

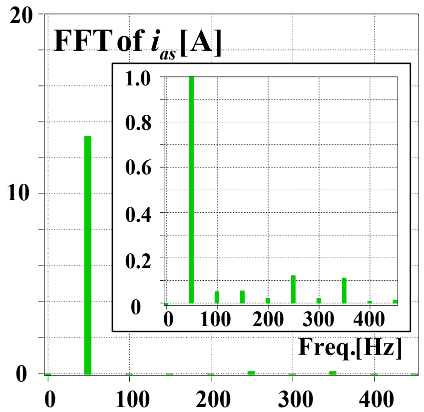

(c)

Fig. 13. Experimental results – FFT of i_{as} in Fig 12 (a) without DTCM, (b) with DTCM1, (c) with DTCM2

compensation method has been built as shown in Fig. 11. The parameters of an induction motor are the same as those in the simulation. The dc-link voltage, switching frequency and dead-time are 320 V, 20 kHz and 3 μs, respectively. The sampling frequency is set to 20 kHz. And the induction motor is controlled by V/F operation (154V/50Hz). The DSP, TMS320F28335 from Texas Instrument, is used for the overall control.

In Fig. 12 (a), the phase current is highly distorted with no compensation. But the distortion of the phase current is remarkably reduced as shown in Fig. 12 (b) by applying the DTCM1. However, the difference between the phase current of DTCM1 and that of DTCM2 in Fig. 12 (c) cannot be found easily from the phase current waveforms because of the impedance of the induction machine.

But the effectiveness of the proposed DTCM methods can be seen from the FFT results of the phase currents as shown in Fig. 13. By applying the DTCM1, the fundamental component and 5^{th}, 7^{th} harmonic components of the phase currents in Fig. 13 (b) are reduced comparing those in Fig. 13 (a). Finally, by DTCM2, as shown in Fig. 13 (c), the distortion has been reduced further.

V. Conclusion

This paper proposed a simple dead-time compensation method based on the simple pole voltage measurement. The pole voltages of the PWM inverter are measured by a simple circuit using eCAP modules in a DSP. The measured voltages are used to compensate the voltage error between commanded voltage and actual output voltage. The compensation method does not rely on any of the phase current information, and it can be applied in low cost adjustable drive system and grid-tied converter system. To improve the performance of the compensation further, another compensation method employing a Proportional and Integral regulator has been also proposed. To verify the validity of the proposed compensation methods, simulation and experiment were carried out based on an induction motor drive system. From simulation and experimental results, it has been verified that the methods reduced the 5^{th}, 7^{th} harmonic components of the phase currents conspicuously.

References

[1] H. Seon-Hwan and K. Jang-Mok, "Dead Time Compensation Method for Voltage-Fed PWM Inverter," *Energy Conversion, IEEE Transactions on,* vol. 25, pp. 1-10, 2010.

[2] C. Jong-Woo and S. Seung-Ki, "A new compensation strategy reducing voltage/current distortion in PWM VSI systems operating with low output voltages," *Industry Applications, IEEE Transactions on,* vol. 31, pp. 1001-1008, 1995.

[3] T. Mannen and H. Fujita, "Dead-Time Compensation Method Based on Current Ripple Estimation," *Power Electronics, IEEE Transactions on,* vol. 30, pp. 4016-4024, 2015.

[4] A. Lewicki, "Dead-Time Effect Compensation Based on Additional Phase Current Measurements," *Industrial Electronics, IEEE Transactions on,* vol. 62, pp. 4078-4085, 2015.

[5] Z. Yue, Q. Wei, and W. Long, "Dead-Time Effect Analysis and Compensation for a Sliding-Mode Position Observer-Based Sensorless IPMSM Control System," *Industry Applications, IEEE Transactions on,* vol. 51, pp. 2528-2535, 2015.

[6] Z. Lanhua, G. Bin, J. Dominic, C. Baifeng, Z. Cong, and L. Jih-Sheng, "A Dead-Time Compensation Method for Parabolic Current Control With Improved Current Tracking and Enhanced Stability Range," *Power Electronics, IEEE Transactions on,* vol. 30, pp. 3892-3902, 2015.

[7] Z. Zhendong and X. Longya, "Dead-Time Compensation of Inverters Considering Snubber and Parasitic Capacitance," *Power Electronics, IEEE Transactions on,* vol. 29, pp. 3179-3187, 2014.

[8] L. Dong-Hee and A. Jin-Woo, "A Simple and Direct Dead-Time Effect Compensation Scheme in PWM-VSI," *Industry Applications, IEEE Transactions on,* vol. 50, pp. 3017-3025, 2014.

[9] K. Dongouk, K. Yong-Cheol, S. Seung-Ki, K. Jang-Hwan, and Y. Rae-Sung, "Suppression of injection voltage disturbance for High Frequency square-wave injection sensorless drive with regulation of induced High Frequency current ripple," in *Power Electronics Conference (IPEC-Hiroshima 2014 - ECCE-ASIA), 2014 International*, 2014, pp. 925-932.

[10] M. A. Herran, J. R. Fischer, S. A. Gonzalez, M. G. Judewicz, and D. O. Carrica, "Adaptive Dead-Time Compensation for Grid-Connected PWM Inverters of Single-Stage PV Systems," *Power Electronics, IEEE Transactions on,* vol. 28, pp. 2816-2825, 2013.

[11] P. Yongsoon and S. Seung-Ki, "A Novel Method Utilizing Trapezoidal Voltage to Compensate for Inverter Nonlinearity," *Power Electronics, IEEE Transactions on,* vol. 27, pp. 4837-4846, 2012.

[12] G. Pellegrino, P. Guglielmi, E. Armando, and R. I. Bojoi, "Self-Commissioning Algorithm for Inverter Nonlinearity Compensation in Sensorless Induction Motor Drives," *Industry Applications, IEEE Transactions on,* vol. 46, pp. 1416-1424, 2010.

[13] T. H. Chin, M. Nakano, and T. Hirayama, "Accurate measurement of instantaneous voltage for power electronics circuits," in *Power Conversion Conference - Nagaoka 1997., Proceedings of the*, 1997, pp. 881-884 vol.2.

[14] S. Yo-Chan, B. Bon-Ho, and S. Seung-Ki, "Sensorless operation of permanent magnet motor using direct voltage sensing circuit," in *Industry Applications Conference, 2002. 37th IAS Annual Meeting. Conference Record of the*, 2002, pp. 1674-1678 vol.3.

[15] T. D. Batzel and M. Comanescu, "Instantaneous voltage measurement in PWM voltage source inverters," in *Electrical Machines and Power Electronics, 2007. ACEMP '07. International Aegean Conference on*, 2007, pp. 168-173.

[16] L. Peretti and M. Zigliotto, "FPGA-based voltage measurements in AC drives," in *Electrical Machines (ICEM), 2010 XIX International Conference on*, 2010, pp. 1-6.